JJMIE

Volume 16, Number 2, March. 2022
ISSN 1995-6665
Pages 283 - 289

Jordan Journal of Mechanical and Industrial Engineering

3D Finite Element Method Simulations on the Influence of Tool Helix Angle in Thin-Wall Milling Process

G. Bolar*

Department of Mechanical & Manufacturing Engineering, Manipal Institute of Technology, Manipal Academy of Higher Education, 576104, Manipal, Karnataka, India

Received 15 JUNE 2021 *Accepted 30 JAN 2022*

Abstract

In the reported work, a three-dimensional (3D) finite element method (FEM) model was developed to assess the effect of cutter helix angle on milling forces and wall deflection considering thin-wall machining of aluminum 2024-T351 alloy. Johnson-Cook (J-C) constitutive law was employed to model the material flow, whereas the material damage was initiated using the Johnson-Cook damage criterion. Work-tool contact was established using a modified Coulombs friction model. The simulations were carried out for a fixed set of process conditions by varying the helix angle, and the predicted results were experimentally validated. Comparing the milling force and deflection values showed that numerical results augured well with the experimentally measured values. The use of an end mill with a higher helix generated lower force values. Also, a smaller magnitude of wall deflection was noted when 45º and 55º helix tools were used. The experimental investigation into the surface roughness indicated improved shearing action and surface finish when high helix tools were employed.

Keywords: Thin-wall machining; helix angle; finite elementsimulation; milling force; deflection; surface roughness.

1. Introduction

The process of machining components having thin sections from a single, monolithic workpiece is known as thin-wall machining. Machining thin-wall parts pose a significant challenge as it requires the maintenance of tight dimensional tolerance, especially in the aerospace and automobile industries. Thin-wall milling is a low productivity process where approximately 90-95 % of the work material is removed during the operation. Moreover, low stiffness often deflects or deforms the thin-wall under machining forces even during CNC milling, where the tool motion is controlled precisely[1]. The in-process deflection under the action of cutting forces results in form error, thereby affecting the accuracy of the machined part.

Research reports on the development of analytical models for cutting force and deflection during thin-wall machining. Ratchev et al. [2] formulated a flexible force model for predicting the thin-wall deflection. A material removal model was included to take care of the changing work geometry and stiffness. Aijun and Zhanqiang [3] analytically predicted the static deformation in thin-wall parts with linear loads as an input.Izamshah et al. [4] developed a prediction methodology for capturing the thin-wall deflection during machining. The model combined the capabilities of statistical analysis and finite element method (FEM). Qi et al. [5] introduced a model for predicting the cutting forces for curved thin-wall milling. The model considered the wall defection and changing workpiece curvature while predicting the cutting forces. Du et al. [6] suggested a methodology to compensate deflection error by computing milling forces and induced deformation. In the model, cutting force was developed considering the plowing and shearing mechanisms. Later, ANSYS parametric design language (APDL) was used to predict deformation. Zhou-Long Li et al. [7] computed the surface errors by considering workpiece and tool deflections. Change in the stiffness of the thin-wall was predicted using a stiffness modification method, while the effect of the tool radial run-out was included for chip thickness calculation and hence the cutting force. Similarly, Altintas et al. [8] outlined a virtual compensation model for predicting the deflection errors in flexible blades using ball-end milling process. Arora et al. [9] put forward a mechanistic force model for in-process deflection prediction while considering the axial and radial engagement of the cutter with the workpiece during thin-wall machining. Chen et al. [10] developed a force-deformation coupling relationship for thin-wall milling process. The contact between the work-tool was defined by discretizing the cutting tool into disk elements. The modification to the instantaneous chip thickness resulted in a new force-deformation coupling relationship to obtain the changing contact conditions and material removal mechanism.

Recent literature includes many research articles on FEM-based numerical studies related to milling. Batista et al. [11] demonstrated a FE methodology for simulating the contour machining process in titanium alloy. Ji et al. [12] carried out research on the helical hole milling process. A 3D numerical model to simulate titanium alloy Ti6Al4V hole milling was developed utilizing commercial FE code ABAQUS/Explicit. The material flow was modeled using the Johnson-Cook (J-C) material model, whereas the material failure and chip formation were outlined utilizing the Johnson-Cook damage model. Coulombs friction law was applied for modeling tool-work interface contact. A

* Corresponding author e-mail: gururaj.bolar@manipal.edu.

3D FE model to simulate titanium alloy Ti6Al4V milling was developed. The workpiece was meshed finely at the cutting region to improve the efficiency of the model. The developed model was made up of 383400 C3D8RT type hexahedral elements. The total simulation time was around 180 hrs [13]. Yue et al. [14]proposed a 3D FE model with the objective of optimizing the cutting force and dimensional accuracy considering corner milling of Cr12MoV steel. The model was developed using a commercial tool DEFORM. An adaptive remeshing technique and an iterative algorithm were adopted to ensure convergence of the developed FE model. Simulated results indicated that spindle speed and feed rate influenced the machining process. An investigation into the thermal stress distribution while machining Cr12MoV mold steel of different hardness using FE analysis was conducted. Upon examination, a significant difference in thermal-stress field was noted due to the variation in material hardness in the transitional domain [15]. 3D FE analysis incorporating equivalent homogeneous material (EHM) model was developed to determine the milling forces at different speeds and feed rates for milling SiCp/Al6063/30P composite [16]. Zhang et al.[17]evaluated the machinability of a sinusoidal surface using FE simulation to determine the cutting temperature and study its influence on surface integrity while machining hardened steel. Chien et al.[18] performed FE based simulation for machining Nickel alloy using a ball end mill. Cutting forces and temperatures were measured and experimentally validated in due process. Gao et al. [19] presented a shoulder milling simulation model by coupling Eulerian-Lagrangian FE method. The simulated results were verified experimentally by machining of Al6061-T6 aluminum alloy. The developed model could accurately predict the cutting force and morphology of chips.

Few researchers have worked on FE modeling of machining processes involving thin-walls. Izamshah et al. [20] presented a transient Lagrangian FE model for simulating thin-wall in-process deflection. 3D FE model was proposed by Cui et al.[21]for simulating thin-wall milling process for machining aluminum alloy 7075-T7451. However, an interaction of single flute was considered for simulation. Huang et al. [22]examined the effect of the FE model of the material and machining induced during machining on thin-wall deformation. The material residual stress was noted to contribute to the wall deformation significantly. Lagrangian formulation-based model successfully simulated the effect of constrained thin-walls on deflection [23]. Material flow behavior and chip formation were simulated by incorporating Johnson-Cook (J-C)material and damage model. Moreover, a thermo-mechanical model was used to determine the milling forces, cutting temperature, chip morphology, and wall deflection [24].

Reviewed literature indicates that FE based investigations are focused on the bulk end milling process. Few research articles focusing on numerical simulations of the thin-wall machining process have been reported. However, a study examining the effect of cutter geometry parameters during thin-wall machining has received scant attention. Therefore, the work focuses on developing a realistic FE model to predict and analyze the impact of cutter helix angle on milling force and in-process deflection during thin-wall milling.

2. Methods and Materials

2.1. 3D Finite Element Modelling

The key to successfully simulating the machining process lies in how the model is developed. The development of the 3D FE model involves modeling of work and tool geometry, assignment of process parameters, boundary conditions, and material properties viz. material flow model, material failure model, and work-tool contact model. The temperature generated during the machining process was ignored in the model to ease computation time and memory. The Lagrangian formulation was used to analyze the transient machining problem. In order to account for large deformation and continuously changing contact, a dynamic explicit time integration scheme was adopted.

2.2. Material Constitutive Model and Material Properties

In aircraft, thin-walls are used as load-bearing structures. These are subjugated to complicated loading behavior during the operation. For fail-free functioning, the structures are desired to have proper rigidity and strength [25]. One material which satisifies the requirement is the aluminum alloys [26, 27]. Specifically, aluminum 2024-T351 is usually used since it possesses high strength and good fatigue resistance. Therefore, in the present study, the analysis is performed on commercial aerospace-grade aluminum 2024-T351 used in the construction of thin-walls. As a material, aluminum 2024-T351 is a solution-treated, cold worked and naturally aged material that is stress relieved by cold stretching [28]. The material is exclusively used in the fabrication of aircraft wings, engine baffles, and fuselage structures [29, 30].

Accurate material modeling is the key to precisely predicting the performance parameters in numerical simulations. Therefore, the material flow was denoted using the material constitutive model proposed by Johnson-Cook (J-C). It is used to model the material flow stress and accounts for the influence of plastic strain, strain rate, process temperature [31]. Accordingly, equivalent plastic flow stress is:

$$\bar{\sigma}_{jc} = \left(A + B\bar{\varepsilon}^{n}\right)\left[1 - C\ln\left(\frac{\dot{\varepsilon}}{\dot{\varepsilon}_{o}}\right)\right]\left(1 - \left(\frac{T_c - T_{room}}{T_{melt} - T_{room}}\right)^{m}\right) \quad (1)$$

where $\bar{\varepsilon}$ is an equivalent plastic strain, $\dot{\varepsilon}$ and $\dot{\varepsilon}_{o}$ are equivalent and reference plastic strain rates, *A* (MPa) the material yield strength, *B* (MPa) the hardening modulus, *C* the strain rate dependency coefficient, *n* is the strain hardening index, *m* is the thermal softening index, T_c is the temperature at the cutting zone and T_{room} and T_{melt} are room and melting temperature. According, J-C parameter values for aluminum alloy 2024-T351 and the workpiece properties are tabulated in Table 1 and Table 2, respectively. Solid carbide end mills have been considered in the study. The end mill is modeled as a rigid body since it is stiffer than the workpiece material.

Table 1. J-C material parameters for aluminum alloy 2024-T351 [32].

A (MPa)	*B* (MPa)	*C*	*n*	*m*
352	440	0.0083	0.42	1

Table 2. Physical properties of workpiece material [32].

Density of material, ρ(kg/m^3)	2700
Elastic modulus, E (GPa)	73
Poisson ratio, v	0.33
Fracture toughness, K_c (MPa $\sqrt{\mathrm{m}}$)	37
Melt temperature, T_{melt} (ºC)	520
Room temperature, T_{room} (ºC)	25

2.3. Material Damage Criterion

The function of a cutting tool is to remove material from the work surface in the form of chips. In FE simulations, the material failure and chip separation must be modeled accordingly. The formation of chips in a numerical simulation is modeled using the damage criterion proposed by Johnson and Cook [33]. The damage model considers the influence of strain, strain rate, and temperature. The damage is initiated when equivalent plastic strain (ε_f) reaches a critical value and is defined by:

$$\varepsilon_f = \left[D_1 + D_2 \exp\left(D_3 \frac{P}{\bar{\sigma}}\right)\right]\left[1 + D_4 \ln\left(\frac{\dot{\varepsilon}}{\dot{\varepsilon}_o}\right)\right]\left(1 + D_5\left(\frac{T_c - T_{room}}{T_{melt} - T_{room}}\right)\right) \quad (2)$$

where D_1-D_5 aredamage constants, P is hydrostatic pressure and $\bar{\sigma}$ is Von Mises equivalent stress. Table 3 lists the J-C damage constants.

Table 3. J-C damage parameters for aluminum alloy 2024-T351 [32].

D_1	D_2	D_3	D_4	D_5
0.13	0.13	-1.5	0.011	0

2.4. Cutting Tool and Workpiece Contact Model

Accurate modeling of the work-tool contact is essential since the metal cutting operation is subjected to high temperature, strain, and strain rate values. Also, predicted values of milling forces, cutting temperature, and tool wear depend on the contact friction at the end milling tool and workpiece interface. Workpiece-tool contact friction is expressed using a modified Coulomb friction model in the present work. Contact between the work and the tool contact consists of two regions, namely, sticking and sliding region. Coulomb's law of friction is applicable in the sliding region, and in the sticking region, frictional stress is equated to shear stress. Relationships are expressed as:

$$\tau = k_{chip} \text{ when } \mu\sigma > k_{chip} \text{ (Sticking region)} \quad (3)$$

$$\tau = \mu\sigma \text{ when } \mu\sigma < k_{chip} \text{ (Sliding region)} \quad (4)$$

Accordingly, the value of the co-efficient of friction was considered as 0.17 [34].

2.5. Cutting Tool and Workpiece Modeling

3D geometric model of the workpiece and the cutting tool was established using commercial FE tool ABAQUS/Explicit. The work-tool assembly and initial mesh configuration are shown in Figure 1. End mills with a rake angle of 8°, a diameter of 16 mm, a clearance angle of 15°, and 4 teeth were used. Helix angle was varied, and tools with the helix of 35°, 45°, and 55° were considered in the study. The initial thickness of the wall was 1 mm. The component was meshed using element type C3D8R. The density of mesh was set higher at the work-tool interaction zone. End mills were meshed using R3D4 rigid elements. Employed cutting variables are listed in Table 4.

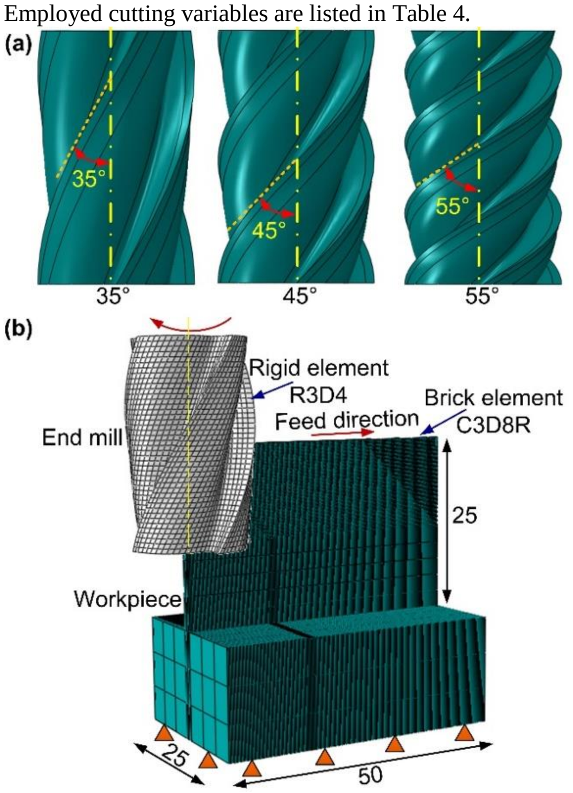

Figure 1. (a) CAD model of cutting tools with different helix angles, (b) Meshed assembly of the tool and workpiece.

Table 4. Process conditions used for simulation.

Spindle speed, n (r/min)	3500
Feed, f_t (mm/tooth)	0.1
Radial cut depth, r_d (mm)	0.3
Axial cut depth, a_d (mm)	12

2.6. Experimental Details

The aluminum workpieces were machined using a three-axis vertical machining center. The 16 mm milling cutter having different helix angles used for the experimental purpose is shown in Figure 2. The workpiece samples were machined to a pre-final dimension,with the wall thickness being 1 mm. The cutting force components were secured using a force dynamometer (*Kistler 9272B*).

The in-process wall deflection was acquired using a linear variable differential transformer (*Solartron: AX/5/S*).

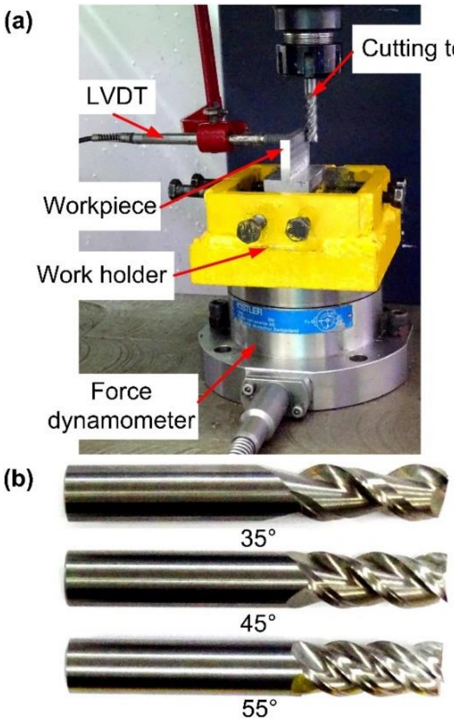

Figure 2. (a) Experimental setup, (b) Cutting tools with different helix angles.

3. Results and Discussion

3.1. Milling Force

Figure 3 shows the comparison of variation in force components F_x (normal) and F_y(feed) for different helix angles. As the values of thrust force component F_z (thrust) was comparatively small, it was neglected in this study. Also, using the experimental setup, the force components were measured and recorded. The predicted force components are represented using solid lines while dotted lines denote the experimentally measured force components. The plots show that the value of force component Fx decreased as the helix angle increased. The predicted mean force F_x when using a 35º helix tool was 82.28 N, whereas, for higher helix tools (45º and 55º), the mean force values were noted to be 66.75 N and 51.1 N, respectively. The variation in the force value is attributed to instantaneous contact points during end milling process [35]. As the number of contact points increases, the volume of work to be machined by each instantaneous cutting edge decreases. This reduces the load on each contact point, reducing the milling force value. The variation in the force component F_y acting along the feed direction was noted to be minimal for the helical angles. Moreover, the predicted and the experimental results for the forces agree well. However, forces predicted by the numerical model were marginally lower than experimental results. Variation is ascribed to assumptions made during the numerical model viz. chatter-free machining, isotropic nature of the work material, tool run-out, etc.[24].

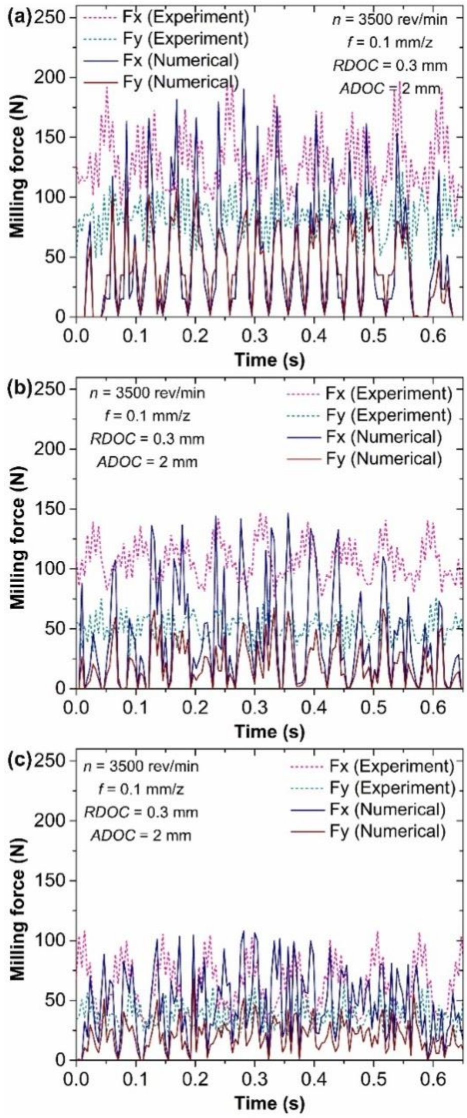

Figure 3. Milling force components vs. helix angle, (a) 35º end mill, (b) 45º end mill, (c) 55º end mill.

3.2. Wall Deflection

In thin-wall machining, in-process deflection results in a loss of form accuracy. Therefore, the in-process deflection was simulated by the developed model. Figure 4 displays the in-process deflection for different helix angles. The deflection magnitude is denoted to decrease with increasing helix angle. The variation is attributed to the normal milling force component (F_x). Higher helix end mill produced lower milling force, resulting in a lower deflection magnitude. Thus end mills with high helix angles are desirable to machine aluminum thin-wall parts with minimum wall deflection. From the plot, it can be seen that the magnitude of deflection obtained experimentally was higher than the values obtained by numerical simulations. The average error between the experimental and numerical values using tools with 35°, 45°, and 55° helix angles was 15%, 16.52%, and 11%, respectively. However, the trends were very well matching.

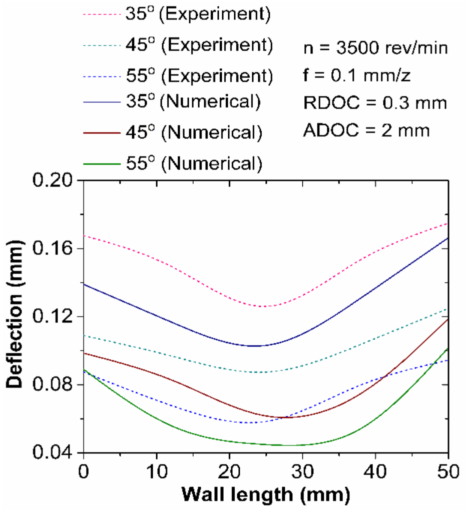

Figure 4. Variation in wall free-end deflection error for different end mill helix angle.

Figure 5 compares form error obtained numerically with the experimental one. Higher in-process deflection during the machining process resulted in a form error. Due to the wall deflection, the material remains uncut (see Figure 6) at the wall free end, producing the wall with a thicker top.

3.3. Formation of Chip and Distribution of Stresses

Figure 7 illustrates the formation of chip and stress distribution during thin-wall milling process. Simulation of chip formation requires fine mesh to provide the desired output, but it increases the simulation time. Therefore, for simulating the chip formation, small portion of the workpiece was finely meshed. The formation of a highly localized primary deformation zone near the tool-workpiece contact region can be noted when the engaging tooth digs into the workpiece. The maximum stress can be observed occurring in the primary deformation zone. Moreover, Figure 7(b-d) gives insight into the post-machining residual stress. As a concluding remark, it can be said that 3D FEM model is a capable tool for simulating the residual stress and complex chip formation phenomenon.

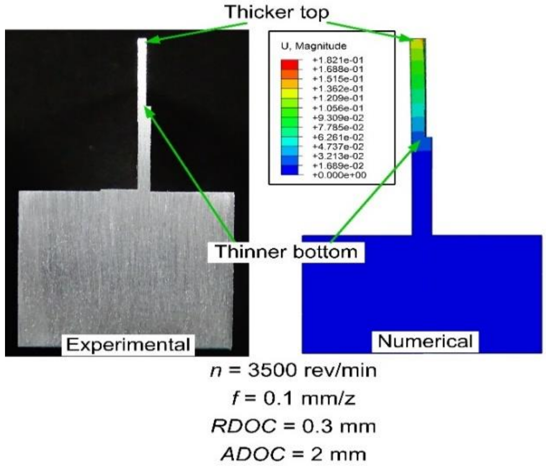

Figure 5. Comparison of form error.

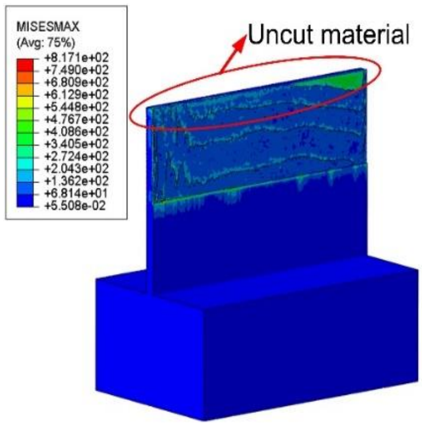

Figure 6. Presence of uncut material after machining.

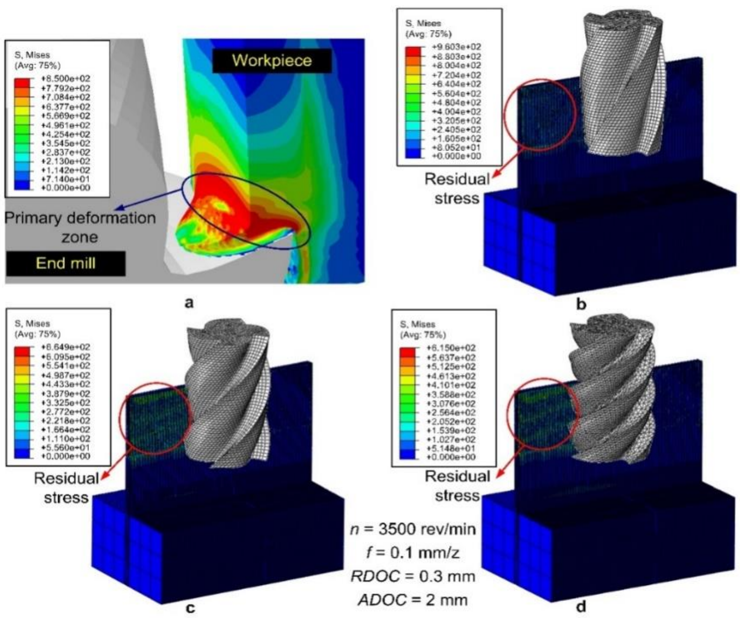

Figure 7. (a) Chip formation and primary deformation zone, (b) Stress developed for 35º tool, (c) Stress developed for 45º tool, (d) Stress developed for 55º tool.

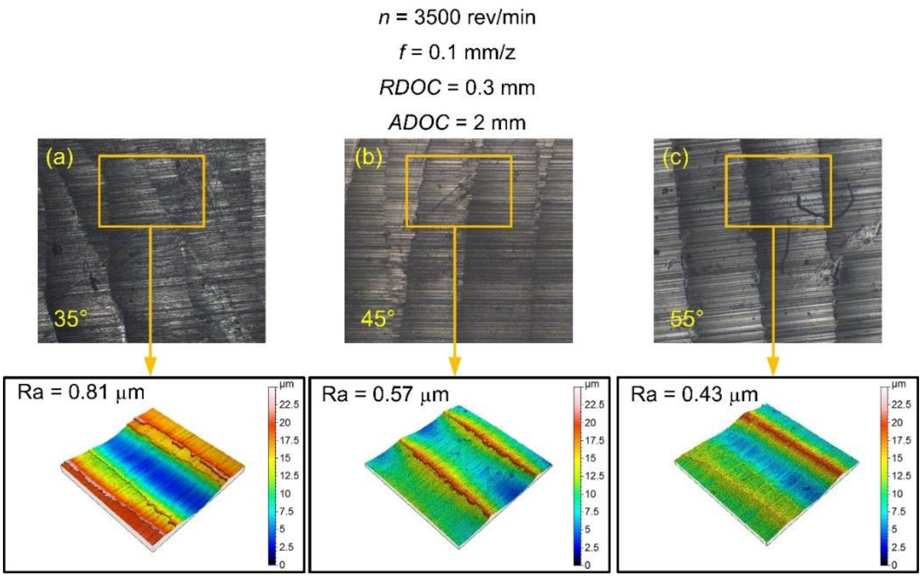

Figure 8. Machined surface topology vs. helix angle (a) 35° helix angle, (b) 45° helix angle, (c) 55° helix angle.

3.4. Experimental Surface Roughness Investigation

The surface of three workpieces experimentally machined using different helix angles was analyzed. Figure 8 displays the topography of surfaces machined using cutters of different helix angles. There was the presence of lay marks on the machined surfaces of all three workpieces, which is typical of the milling operation. The work sample machined with an end mill having a 35° helix angle showed deformed lay marks due to the excessive force developed. An enhancement in the machining surface finish was noted as the tool helix angle increased. Use of end mills having helix angles varying between 45°-55° produced surface with uniform lay marks, which can be attributed to the effective shearing action by the sharp cutting edges.

4. Conclusions

In the presented work, a realistic 3D transient FE model was developed to evaluate the effect of tool helix angle during thin-wall milling. The developed model incorporated material constitutive model, material damage criterion, and contact model to develop a realistic 3D FE simulation for the complex thin-wall milling process. The developed model predicted the milling force components Fx (normal) and Fy (feed). The results clearly show that the helix angle was influencing the normal force component Fx. The magnitude of force component was higher with the use of a cutter with 35º. Moreover, the value of force components predicted using FE model augured well with experimental results. Results also indicate that the helix angle of the end mills influences the wall deflection. Deflection magnitude along the free end of the wall was higher in the case where the 35º helix tool was used. The lower deflection was observed with the use ofhigher helix cutters (45º and 55º). Using tools with a high helix tool generated a lower force value, resulting in a lower magnitude of wall deflection. The use of end mills having helix angles varying between 45°-55° helped in an effective shearing action, thereby producing a machined surface with an improved finish. The results confirmed that FE tool is adept in predicting the milling force, wall deflection, and form error.It is also successful in simulating the chip formation phenomenon with the assistance of J-C material and the damage model.The model can be further advanced to include the phenomenon of heat generation and study the influence of tool geometry parameters viz. rake angle and tool diameter of wall deflection and milling force.

References

[1] M. Farouk, R. Mohamed, S. Fethi, "Development of A New Technique for Modeling and Optimizing Manufacturing Errors for Cn Machine Tools". Jordan Journal of Mechanical & Industrial Engineering, Vol. 14, 2020, 381–386.

[2] S. Ratchev, W. Huang, S. Liu, A.A. Becker, "Modeling and simulation environment for machining of low-rigidity components". Journal of Materials Processing and Technology, Vol. 153–154, 2004, 67–73.

[3] T. Aijun, L. Zhanqiang, "Deformations of thin-walled plate due to static end milling force". Journal of Materials Processing and Technology, Vol. 206, 2008, 345–351.

[4] R. Izamshah, J.P.T. Mo, S. Ding, S."Hybrid deflection prediction on machining thin-wall monolithic aerospace components". Proceedings of the Institution of Mechanical Engineers, Part B: Journal of Engineering Manufacture, Vol. 226, 2012, 592–605.

[5] H. Qi, Y. Tian, D. Zhang, "Machining forces prediction for peripheral milling of low-rigidity component with curved geometry". The International Journal of Advanced Manufacturing Technology, Vol. 64, 2013, 1599–1610.

[6] Z. Du, D. Zhang, H. Hou, S.Y. Liang, S. Y. "Peripheral milling force induced error compensation using analytical force model and APDL deformation calculation". The International Journal of Advanced Manufacturing Technology, Vol. 88, 2017, 3405–3417.

[7] Z.L. Li, O. Tuysuz, L.M. Zhu, Y. Altintas,"Surface form error prediction in five-axis flank milling of thin-walled parts". International Journal of Machine Tools and Manufacture, Vol. 128, 2018, 21–32.

[8] Y. Altintas, O. Tuysuz, M. Habibi, Z.L. Li, "Virtual compensation of deflection errors in ball end milling of flexible blades". CIRP Annals, 67, 2018, 365–368.

[9] N. Arora, A. Agarwal, K.A. Desai, "Modelling of static surface error in end-milling of thin-walled geometries".

International Journal of Precision Technology, Vol. 8, 2019, 107–123.

[10] Z. Chen, C. Yue, S.Y. Liang, X. Liu, H. Li, X. Li, "Iterative from error prediction for side-milling of thin-walled parts". The International Journal of Advanced Manufacturing Technology, Vol. 107, 2020, 4173–4189.

[11] M. Batista, A. Morales, A. Gómez-Parra, J. Salguero, F.J. Puerta, M. Marcos, "3D-FEM Based Methodology for Analysing Contour Milling Processes of Ti Alloys". Procedia Engineering, Vol. 132, 2015, 1136–1143.

[12] C. Ji, Y. Li, X. Qin, Q. Zhao, D. Sun, Y. Jin, "3D FEM simulation of helical milling hole process for titanium alloy Ti-6Al-4V". The International Journal of Advanced Manufacturing Technology, Vol. 81, 2015, 1733–1742.

[13] H.B. Wu, S.J. Zhang, "3D FEM simulation of milling process for titanium alloy Ti6Al4V". The International Journal of Advanced Manufacturing Technology, Vol. 71, 2014, 1319–1326.

[14] C. Yue, C. Huang, X. Liu, S. Hao, J. Liu, "3D FEM Simulation of Milling Force in Corner Machining Process". Chinese Journal of Mechanical Engineering. Vol. 30, 2017, 286–293.

[15] W. Zhang, C. Cheng, X. Du, X. Chen,"Experiment and simulation of milling temperature field on hardened steel die with sinusoidal surface". International Journal on Interactive Design and Manufacturing. Vol. 12, 2018, 345–353.

[16] X. Chen, L. Xie, X. Xue, X. Wang, "Research on 3D milling simulation of SiCp/Al composite based on a phenomenological model". The International Journal of Advanced Manufacturing Technology, Vol. 92, 2017, 2715–2723.

[17] W. Zhang, F. He, T. Wu, C. Du, H. Liu,"3D numerical simulation on thermal-stress distribution of hardened steels workpiece assembled with different hardness". International Journal on Interactive Design and Manufacturing, Vol. 11, 2017, 559–568.

[18] S.E.M. Chien, M.M. Reddy, V.C.C. Lee, D. Sujan, "The Study of Coated Carbide Ball End Milling Tools on Inconel 718 Using Numerical Simulation Analysis to Attain Cutting Force and Temperature Predictive Models at the Cutting Zone". Materials Science Forum, Vol. 882, 2017, 28–35.

[19] Y. Gao, J.H. Ko, H.P. Lee,"3D coupled Eulerian-Lagrangian finite element analysis of end milling". The International Journal of Advanced Manufacturing Technology, Vol. 98,2018, 849–857.

[20] R.A. Izamshah, J. Mo, S.L. Ding,"Finite Element Analysis of Machining Thin-Wall Parts". Key Engineering Materials, Vol. 458, 2010, 283–288.

[21] K.H. Cui, C.Z. Ren, G. Chen, "Numerical Simulation for Peripheral Milling of Aero-Aluminum Alloy Based on 3D FE Model". Key Engineering Materials, Vol. 589-590, 2013, 3–7.

[22] X. Huang, J. Sun, J. Li, "Finite element simulation and experimental investigation on the residual stress-related monolithic component deformation". The International Journal of Advanced Manufacturing Technology, Vol. 77, 2015, 1035–1041.

[23] S.N. Joshi, G. Bolar, "Three-Dimensional Finite Element Based Numerical Simulation of Machining of Thin-Wall Components with Varying Wall Constraints". Journal of The Institution of Engineers (India): Series C, Vol. 98, 2017, 343-352.

[24] G. Bolar, S.N. Joshi,"Three-dimensional numerical modeling, simulation and experimental validation of milling of a thin-wall component".Proceedings of the Institution of Mechanical Engineers, Part B: Journal of Engineering Manufacture.Vol. 231, 2017, 792–804.

[25] P. Bałon, E. Rejman, A. Świątoniowski, B. Kiełbasa, R. Smusz, J. Szostak, J. Cieślik, L. Kowalski, "Thin-walled Integral Constructions in Aircraft Industry". Procedia Manufacturing, Vol. 47, 2020, 498–504.

[26] N. Gharaibeh, M. AlAjlouni, A. Al-Rousan, "Olive Mill Wastewater as Cutting Fluids: Effect on Surface Roughness of Aluminum". Jordan Journal of Mechanical & Industrial Engineering, Vol 12, 2018,161–166.

[27] Y. Liu, L. He, L., S. Yuan, "Wear Properties of Aluminum Alloy 211z.1 Drilling Tool". Jordan Journal of Mechanical & Industrial Engineering, Vol. 15, 2021,59–63.

[28] A. Gariépy, F. Bridier, M. Hoseini, P. Bocher, C. Perron, M. Lévesque, "Experimental and numerical investigation of material heterogeneity in shot peened aluminium alloy AA2024-T351". Surface and Coatings Technology, Vol. 219, 2013, 15–30.

[29] C.A. Rodopoulos, A.T. Kermanidis, E. Statnikov, V. Vityazev, O. Korolkov, "The effect of surface engineering treatments on the fatigue behavior of 2024-T351 aluminum alloy". Journal of Materials Engineering and Performance, Vol. 16, 2007, 30–34.

[30] O.S. Zaroog, A. Ali, B.B. Sahari, R. Zahari, "Modeling of residual stress relaxation of fatigue in 2024-T351 aluminium alloy". International Journal of Fatigue, Vol. 33, 2011, 279–285.

[31] G.R. Johnson, W.H. Cook, (1983) "A constitutive model and data for materials subjected to large strains, high strain rates, and high temperatures". Proceedings of the 7th International Symposium on Ballistics, Hague, the Netherlands,1983.

[32] T. Mabrouki, F. Girardin, M. Asad, J.F. Rigal,"Numerical and experimental study of dry cutting for an aeronautic aluminium alloy (A2024-T351)". International Journal of Machine Tools and Manufacture,Vol. 48, 2008, 1187–1197.

[33] G.R. Johnson, W.H. Cook,"Fracture characteristics of three metals subjected to various strains, strain rates, temperatures and pressures". Engineering fracture mechanics, Vol. 21, 1985, 31–48.

[34] M. Madaj, M. Píška, "On the SPH orthogonal cutting simulation of A2024-T351 alloy". Procedia CIRP, Vol. 8, 2013, 152–157.

[35] P. Baowan, C. Saikaew, A. Wisitsoraat,"Influence of helix angle on tool performances of TiAlN- and DLC-coated carbide end mills for dry side milling of stainless steel". The International Journal of Advanced Manufacturing Technology, Vol. 90, 2017, 3085–3097.